AAPS PharmSciTech, Vol. 11, No. 2, June 2010 (© 2010)
DOI: 10.1208/s12249-010-9461-5

Research Article

Characterization of Cimetidine–Piroxicam Coprecipitate Interaction Using Experimental Studies and Molecular Dynamic Simulations

Vimon Tantishaiyakul,[1,3] Krit Suknuntha,[1] and Visit Vao-Soongnern[2]

Received 16 November 2009; accepted 13 May 2010; published online 29 May 2010

Abstract. The crystalline states of cimetidine and piroxicam, when coprecipitated from solvents containing 1:1 mole ratio, were transformed to amorphous states as observed using powder X-ray diffraction (PXRD). Amorphous forms of drugs generally exhibit higher water solubility than crystalline forms. It is therefore interesting to investigate the interactions that cause the transformation of both the crystalline drugs. Intermolecular interactions between the drugs were determined using Fourier-transform infrared spectroscopy (FTIR) and solid-state ^{13}C CP/MAS NMR. Molecular dynamic (MD) simulation was performed for the first time for this type of study to indicate the specific groups involved in the interactions based on radial distribution function (RDF) analyses. RDF is a useful tool to describe the average density of atoms at a distance from a specified atom. FTIR spectra revealed a shift of the C≡N stretching band of cimetidine. The ^{13}C CP/MAS NMR spectra indicated downfield shifts of C_{11}, C_{15} and C_7 of piroxicam. RDF analyses indicated that intermolecular interactions occurred between the amide oxygen atom as well as the pyridyl nitrogen of piroxicam and H-N_3 of cimetidine. The hydrogen atom (O–H) at C_7 interacts with the N_1 of cimetidine. Since the MD simulation results are consistent with, and complementary to the experimental analyses, such simulations could provide a novel strategy for investigating specific interacting groups of drugs in coprecipitates, or in amorphous mixtures.

KEY WORDS: ^{13}C CP/MAS NMR; cimetidine; molecular dynamics; piroxicam; X-ray powder diffractometry.

INTRODUCTION

Piroxicam (P), a nonsteroidal anti-inflammatory drug (NSAID), is commonly used to relieve pain, inflammation and stiffness caused by arthritis. It also exhibits chemopreventive and antitumor effects (1,2). NSAIDs are frequently associated with high incidences of gastroenteropathy, ranging from mild gastric upset to life-threatening ulceration and hemorrhage (3). Cimetidine (C), a H_2-receptor antagonist, is commonly used in the prevention and treatment of duodenal and gastric ulcers (4). It can reduce gastric ulcers associated with NSAID therapy and also increase the anti-inflammatory activity (5). Moreover, it also exhibits antitumor activity on gastrointestinal cancers (6,7).

The concomitant administration of cimetidine and piroxicam does not result in any impairment of the efficacy of piroxicam, or cause any adverse effect (8), but co-administration of cimetidine can result in an increase in the plasma concentrations of piroxicam (9). The preparation of binary mixtures of some drugs has been reported to be accompanied by a change in the crystalline structures of the starting drugs (10,11). Therefore, the coprecipitate and a physical mixture of piroxicam and cimetidine were experimentally prepared with a C:P mole ratio of 1:1. According to our preliminary study, both cimetidine and piroxicam in this coprecipitate were transformed to amorphous forms. Generally, an amorphous drug exhibits maximal solubility enhancement as compared to its crystalline form (12). This higher solubility and dissolution advantage can increase bioavailability of poorly water-soluble drugs (13,14). Thus, amorphous drugs have attracted a great deal of attention from pharmaceutical scientists. Regarding the solubility of crystalline cimetidine and piroxicam, the former is soluble in water whereas the latter exhibits low water solubility. Therefore, amorphous piroxicam is needed, and several preparation methods have been developed over the past decade, mostly using polymers and β-cyclodextrin (15-18). In the present study, however, amorphous piroxicam was prepared by coprecipitation with cimetidine. Following the preparation and characterization of this coprecipitate at 1:1 C:P mole ratio, we also systematically investigated other mole ratios of cimetidine and piroxicam coprecipitates (19). The dissolution of these coprecipitates was demonstrated to be substantially higher than that of drug alone.

Investigation interaction networks between drug–drug or drug–excipients/carriers, is important to develop and/or optimize stability of amorphous systems. Generally, the combination of many analytical techniques is required to characterize the complex interactions in amorphous solid states. These techniques include PXRD (19,20), FTIR

[1] Department of Pharmaceutical Chemistry, Faculty of Pharmaceutical Sciences, Prince of Songkla University, Hat Yai, Songkhla 90112, Thailand.
[2] School of Chemistry, Institute of Science, Suranaree University of Technology, Nakhon Ratchasima, 30000, Thailand.
[3] To whom correspondence should be addressed. (e-mail: vimon.t@psu.ac.th)

(16,19), differential scanning calorimetry (21), and solid-state NMR (18,22). Besides these experimental techniques, computational methods have also proven to be useful tools in the investigation of drug properties, and particularly in the examination of intra- and intermolecular interactions between different materials (23,24). MD is a type of computer simulation in which atoms and molecules are allowed to interact for a period of time. The information of their motion is gathered and used to deduce the bulk properties of material. MD is generally used in the study of proteins and material sciences. Recently, MD simulations carried out using the amorphous cell module have been employed in various studies, such as prediction of solubility parameters of organic molecules (25), drug transport through adhesive polymers (26) and diffusion/permeation of small molecules/gases in membranes (27,28). Furthermore, MD simulations were successfully used for investigating the specific groups that interact with each other in polymer blends based on RDF analyses, which reveals the average density of atoms at a distance from a specified atom (23,24). MD simulations may be able to serve as a complement to conventional experimental protocols. In this study, FTIR and solid-state ^{13}C CP/MAS NMR experiments were performed to determine the crystalline forms, and the nature of the interaction between cimetidine and piroxicam. Additionally, MD simulations were performed to determine which specific groups were involved in these intermolecular interactions.

MATERIALS AND METHODS

Materials

Piroxicam was obtained from Vertex Chemicals (Hong Kong), and found to correspond to form II (29,30). Cimetidine was purchased from Sigma (St. Louis, MO, USA) which was the A polymorph. The C polymorphic form of cimetidine was prepared according to a previously described method (31). Other reagents were purchased from Aldrich (St. Louis, MO, USA) and Fisher Scientific (Fairlawn, NJ, USA).

Preparation of Cimetidine–Piroxicam Binary Mixtures

In the preparation of a coprecipitate with a C:P mole ratio of 1:1, a solution of cimetidine form A (2 g) in methanol (20 ml) was added to a stirred solution of piroxicam form II (2.63 g) in acetonitrile (100 ml). The resulting mixture was stirred for 2 h and then evaporated under reduced pressured at 40°C. The residual solvent was removed under vacuum for 2 days. Physical mixtures (PM) were prepared by thoroughly mixing the 0.05–0.25 mm particle size fractions of cimetidine form A (2 g) and piroxicam form II (2.63 g) in a mortar.

X-ray Powder Diffraction Measurements

PXRD patterns were obtained using a Philips PW 3710 diffractometer with Cu-Kα radiation, collimated by a 0.08° divergence slit and a 0.2° receiving slit and scanned at a rate of 2.4°/min over the 2θ range of 5.0–60.0°.

Fourier-Transform Infrared Spectroscopic Measurements

FTIR spectra were obtained on a PerkinElmer Spectrum One spectrometer. A polystyrene filter was used to check the spectrophotometer calibration. Samples were prepared as KBr discs. In the attempt to obtain an acceptable signal/noise ratio, 32 scans acquired using the FTIR spectrometer with a resolution of 4 cm^{-1} were averaged.

Solid-State ^{13}C CP/MAS NMR Measurements

The NMR experiments were conducted using a Bruker Avance 300 NMR spectrometer operating at 75.51 MHz for ^{13}C using standard 4 mm cross-polarization magic angle-spinning probes (CP/MAS). The samples were spun at the magic angle at a rate of 10,620 Hz with a total number scans of 10,000 thereby eliminating spinning side band interference. A contact time of 5.0 ms was used, and a recycle delay between scans for all the samples was 3 s. The ^{13}C chemical shifts were referenced with respect to tetramethylsilane (=0 ppm), using solid adamantine as a secondary standard.

Computational Method

Molecular dynamics simulations of the coprecipitate with 50 molecules of each drug were performed using Materials Studio 4.2 (Accelrys, Inc., USA) on a Core 2 Quad computer. The COMPASS force field was employed for all calculations. This forcefield is based on the *ab initio* consistent forcefield CFF91, and can be used for a broad range of drugs including polymers, polysaccharides, and organic molecules. Each drug was minimized using the Discover module, and the amorphous phase of cimetidine/piroxicam system was built inside a box with periodic boundary conditions constructed using the amorphous cell module of the Materials Studio. The density of each system was estimated from densities of the pure drugs. Literature values were averaged to obtain the density value of 1.3 g/cm^3 for cimetidine used in this study (32). The ^{13}C CP/MAS spectra acquired in the present study of the amorphous form of piroxicam were found to be similar to that of piroxicam form I. Therefore, literature density values of piroxicam form I were averaged to obtain the value of 1.47 g/cm^3 used in this study (33). Thus, the initial simulation cell densities for this coprecipitate was 1.40 g/cm^3 with dimensions of 32.59×32.59×32.59 Å.

The amorphous assembly was energy minimized using the steepest descent method, followed by the conjugate gradient method with a convergence level of 0.01 kcal/mol/Å. Atom-based cutoff of 15.50 Å and a switching function with the spline and buffer widths of 5 and 2 Å, respectively, were applied to evaluate nonbonded interactions. Due to the fact that the density of the amorphous coprecipitate is different from those of the crystalline structures of the starting pure drugs, the simulations were therefore carried out with NPT ensemble (constant particle numbers, pressure, and temperature), using the Andersen and Berendsen methods to control temperature and pressure, respectively, for density adjustment. These isothermal–isobaric (NPT) simulations were performed at atmospheric pressure as previously described (34). Subsequently, the NVT (constant number of molecules, volume and temperature) simulations

were conducted using a short-run relaxation cycle to relax the bulk structure as previously described (35). The cycle consists of a 0.02 ns NVT dynamics simulation at 800 K, followed by an energy minimization run, 0.02 ns NVT at 600 K, and minimization, and then another 0.02 ns dynamics at 800 K and energy minimization. The NVT simulation was then performed for a period of 1 ns at 298 K with a time step of 1 fs. When equilibrium was reached, radial distribution functions (RDFs), g(r), were calculated.

RESULTS AND DISCUSSION

X-ray Powder Diffraction

The molecular structures and numbering system for cimetidine and piroxicam are presented in Fig. 1. PXRD measurements were employed to investigate the changes in crystallinity and the polymorphic form of the samples upon coprecipitation or physical mixing. Figure 2 shows the PXRD patterns of cimetidine form A, piroxicam form II, as well as the coprecipitate and the physical mixture of both drugs. The coprecipitate prepared from cimetidine form A and piroxicam form II does not show any peak in its PXRD profile. This indicates that both cimetidine and piroxicam in this coprecipitate are in an amorphous state. The PXRD pattern of the physical mixture shows that the features of cimetidine and piroxicam are retained, indicating that interaction between these two drugs are not occurring in the physical mixture.

FTIR Analyses

The FTIR spectra of cimetidine forms A and C, piroxicam forms I and II, as well as the coprecipitate and physical mixture of cimetidine form A and piroxicam form II are presented in Fig. 3. The FTIR spectra of piroxicam forms I and II show prominent N–H stretching peaks at 3339 and 3393 cm^{-1}, respectively (29,36). Those of cimetidine forms A and C display major peaks of C≡N at 2178 and 2166 cm^{-1}, respectively (37). The C≡N stretching band of the cimetidine starting material (form A) at 2178 cm^{-1} is shifted to 2166 cm^{-1} in the coprecipitate. One possible interpretation of this observation is that cimetidine in the amorphous form

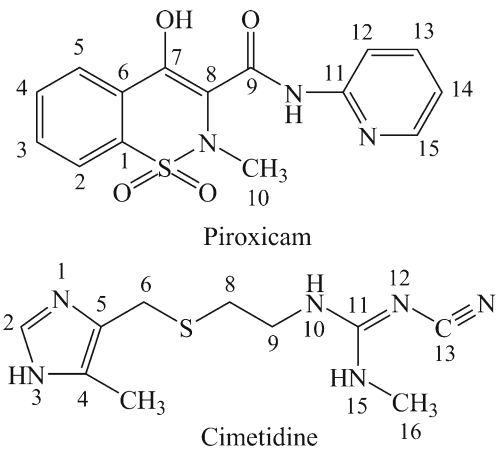

Fig. 1. Structures of piroxicam and cimetidine

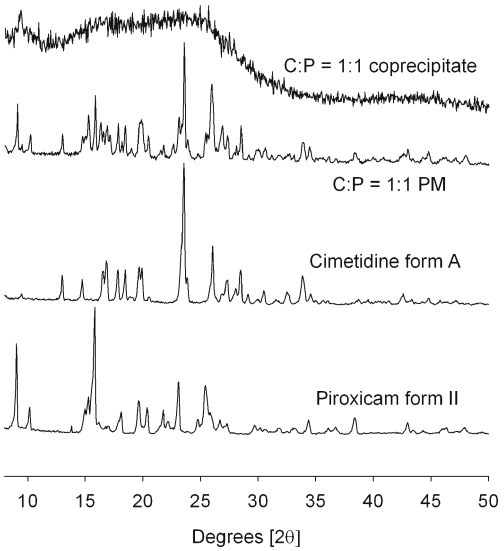

Fig. 2. PXRD patterns of cimetidine (C) form A, piroxicam (P) form II, and physical mixture (PM) and coprecipitate of C:P at 1:1 mole ratio

possesses some of the characteristics of cimetidine form C. The N–H stretching band was not observed for piroxicam in the coprecipitate. This is possibly due to the formation of strong hydrogen bond of this amide hydrogen. Furthermore, the identical FTIR spectra for piroxicam form II and cimetidine form A were obtained when the single drug was treated using the same procedure as used for coprecipitate preparation. Thus, the change of the crystal structure of both drugs in the coprecipitate is not caused by the process of coprecipitate preparation. FTIR spectra of the physical mixture shows a summation of peaks of both drugs, the N–

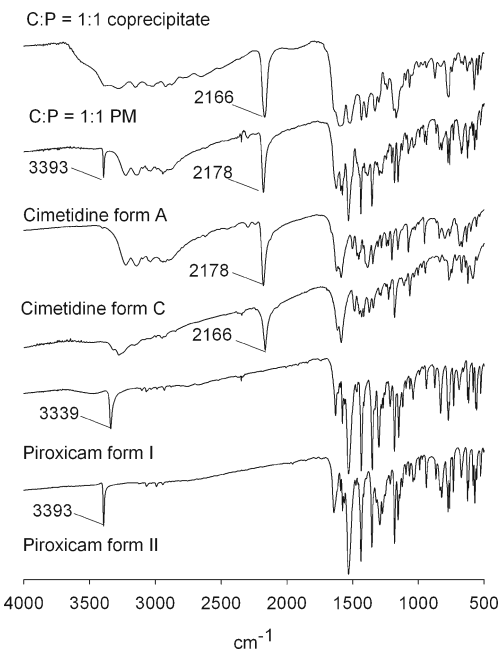

Fig. 3. FTIR spectra of cimetidine (C) forms A and C, piroxicam (P) forms I and II, and physical mixture (PM) and coprecipitate of C:P at 1:1 mole ratio

H peak of piroxicam and the C≡N band of cimetidine remain at the same wavenumbers of the starting drugs. This is consistent with the PXRD analysis and confirms that intermolecular interaction between these two drugs does not take place in their physical mixtures.

Solid-State ^{13}C CP/MAS NMR Analyses

The ^{13}C CP/MAS NMR spectra of piroxicam forms I and II, cimetidine forms A and C are shown in Fig. 4. These spectra are similar to those previously reported for polymorphic forms of cimetidine (38) and piroxicam (18,29, 39). The signals were assigned as described in literature in accordance with the numbering systems of cimetidine and piroxicam structures presented in Fig. 1. According to the FTIR results, the coprecipitate contains some cimetidine form C features. The ^{13}C CP/MAS NMR spectra of the coprecipitate (Fig. 5) shows two peaks at 152.6 and 148.7 ppm, which are similar to those of piroxicam form I. The ^{13}C CP/MAS NMR spectra of piroxicam form I and cimetidine form C are, therefore, used to examine the interaction between piroxicam and cimetidine in the coprecipitate. The spectrum of the coprecipitate (Fig. 5) shows broad spectral features which signify amorphous materials. The resonance signals of C_{11} and C_{15} at 150.4 and 147.2 ppm, respectively, of piroxicam form I is slightly shifted downfield to 152.6 and 148.7 ppm, respectively, in the coprecipitate (Fig. 5). This indicates that the pyridyl nitrogen of piroxicam may be involved in hydrogen bonding with a proton donor of cimetidine. Alternatively, piroxicam in the coprecipitate may be converted to a zwitterionic structure which contains a positive charge on the pyridyl nitrogen. The ^{13}C chemical shifts of the uncharged and zwitterionic forms of piroxicam have previously been reported in the literature (18,40). The chemical shifts of C_{11} and C_{15} in a solution (*N*,*N*-dimethylformamide) for the uncharged form were observed

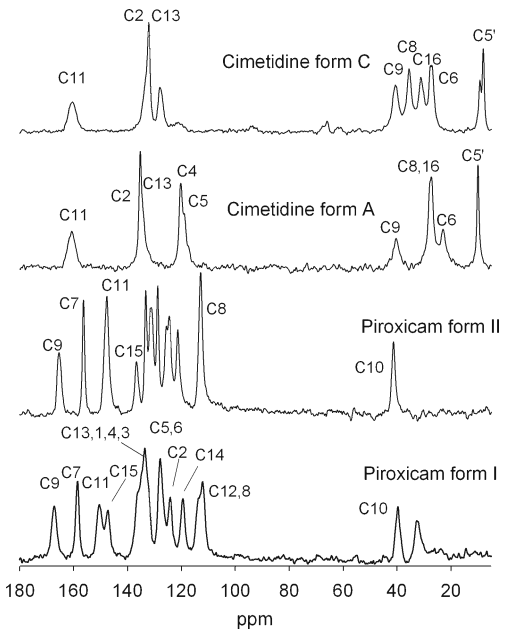

Fig. 4. ^{13}C NMR spectra of cimetidine forms A and C and piroxicam forms I and II

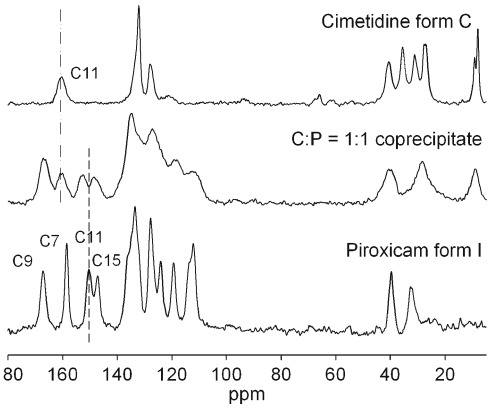

Fig. 5. ^{13}C NMR spectra of piroxicam (P) form I, cimetidine (C) form C and coprecipitate of C:P at 1:1 mole ratio

at δ 151.3 and 149.2 ppm, respectively, and those for the zwitterionic form appeared at δ 150.5 and 138.0 ppm, respectively (40). The distance (3.9 ppm) between the peak position of C_{11} (152.6 ppm) and C_{15} (148.7 ppm) for the coprecipitate is more similar to that of the uncharged form (2.1 ppm) than that of the zwitterionic form (12.5 ppm). In addition, the comparable distance (10.4 ppm) between peak position of C_{11} (149.4 ppm) and C_{15} (139.0 ppm) for the piroxicam monohydrate, assumed to exist as zwitterionic structure (18,40), was also reported. For piroxicam form I and piroxicam in the coprecipitate, these peaks were not resolved as shown in Fig. 5. These patterns of NMR spectra suggest that piroxicam in the coprecipitate is in the uncharged form, and the slight downfield shift of C_{11} and C_{15} may result from hydrogen bonding of the pyridyl nitrogen with a proton donor group.

The C_7 signal at 158.4 ppm of piroxicam is shifted downfield to 167.2 ppm, and appears as a broad peak co-mixed with the C_9 peak for piroxicam in the coprecipitate (Fig. 5). Alternatively, this C_7 signal may have shifted downfield to 160.3 ppm, and is perhaps overlapped with the C_{11} signal of cimetidine. This downfield shift of C_7 signal might suggest that the oxygen atom of the OH group of piroxicam functions as a proton acceptor and donates electrons to the hydrogen atom of the cimetidine molecule. Another possibility is that the amide oxygen atom at C_9 (C═O) may interact with a proton donor of cimetidine via the facilitation of electron delocalization from C_7. As shown in Fig. 5, the chemical shifts for the C_{11} of cimetidine form C are detected at 160.3 ppm. A peak at 160.3 ppm is also observed in the spectra of the coprecipitate. The fact that this signal remains at the same position in the NMR spectrum of the coprecipitate suggests that nitrogen atoms connected to C_{11}, or hydrogen atoms attached to these nitrogen atoms, do not interact with piroxicam. Other signals from cimetidine are blended with the resonance signals from piroxicam, and appear as complex broad peaks in the coprecipitate. Therefore, it is relatively complicated to elucidate other possible groups of cimetidine that interact with those of piroxicam.

MD Simulations and RDF Analyses

MD simulations of the amorphous coprecipitate were carried out to investigate the specific groups of piroxicam and

cimetidine that might be interacting with each other based on the RDF analyses. An amorphous cell containing 50 molecules of each drug is shown in Fig. 6. The RDFs were analyzed in the interval of simulations where the simulation displays a stable behavior, i.e., from 0.4 to 1 ns (Fig. 7). These MD simulations can be used in conjunction with the experimental methods to identify molecular interactions between piroxicam and cimetidine in the coprecipitate.

The most stable N_3–H tautomer of cimetidine (41) and piroxicam in an uncharged form (Fig. 1) were used for MD simulations. Figure 8 shows the RDF calculations for the oxygen atom at C_7 of piroxicam and the proton donor group of cimetidine. No peak is found for this RDF analysis, indicating that the oxygen atom at C_7 does not interact with cimetidine. However, a pronounced peak at 1.95 Å with a g(r) function of 3.18 was observed for the amide oxygen atom at C_9 (C=O) of piroxicam and H–N_3 of cimetidine (Fig. 9). According to ^{13}C CP/MAS NMR spectra, the chemical shift of C_9 of piroxicam form I and that in the coprecipitate remains almost at the same position (Fig. 5). The downfield shift of piroxicam C_7 in conjunction with these RDF calculations indicate that the hydrogen bond between the amide oxygen atom at C_9 (C=O) of piroxicam and the proton donor of cimetidine (H–N_3) is facilitated by electron delocalization from C_7. Furthermore, a peak at 1.85 Å with g (r) function of 1.48 was found for N-pyridine of piroxicam and H–N_3 of cimetidine (Fig. 9). This RDF analysis is consistent with the ^{13}C CP/MAS NMR which shows slight downfield shifts of the carbon atoms (C_{11} and C_{15}) attached to the pyridyl nitrogen atom. These studies indicate that intermolecular hydrogen bonding takes place between the pyridyl nitrogen of piroxicam and the proton donor at N_3 (H–N_3) of cimetidine. Apart from the interaction with the proton donor H–N_3 of cimetidine, no peak was found for the RDF analyses of the amide oxygen atom at C_9 (C=O), or the N-pyridine of piroxicam for the other proton donors of cimetidine. This suggests that H–N_3 of imidazole ring of cimetidine is the only proton donor group that interacts with the proton acceptor groups of piroxicam.

To investigate the interaction of the proton donor groups of piroxicam, the RDF calculations for the hydrogen atoms of

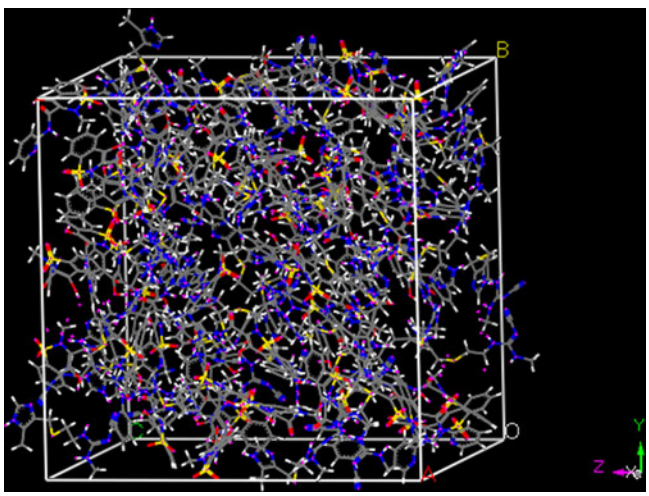

Fig. 6. An amorphous cell containing 50 molecules of each piroxicam and cimetidine

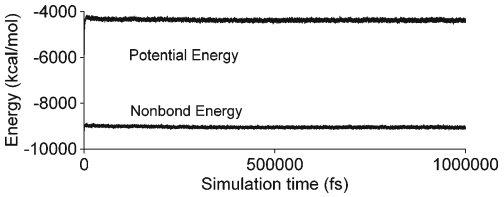

Fig. 7. Potential and nonbond energy *vs* simulation time of 1 ns

OH–C_7 and amide function at C_9 (N–H) of piroxicam with proton acceptors of cimetidine were analyzed. A major peak at 1.75 Å with g(r) function of 2.67 was found for hydrogen of OH-C_7 and N_1 cimetidine (Fig. 10). No other prominent peak was detected from these RDF analyses, suggesting that the hydrogen atom of the OH–C_7 does not interact with the other proton acceptors from cimetidine. Similarly, major peaks were not observed for RDF analyses for the amide hydrogen atom at C_9 (N–H) and the proton acceptors of cimetidine (Fig. 11). This suggests that no interaction occurs between the hydrogen atom of amide function (N–H) of piroxicam and the proton acceptors of cimetidine. However, the N–H stretching vibration of piroxicam at 3393 or 3339 cm^{-1} was not observed in the FTIR spectrum of the coprecipitate (Fig. 3). This N–H stretching band for amorphous piroxicam was also not detected in previous studies (15-17). The interactions between piroxicam and cimetidine may cause change of the molecular conformation of piroxicam. The amide hydrogen is able to form intermolecular hydrogen bond with the pyridyl nitrogen since a peak at 2.05 Å with g(r) function of 2.36 was observed for amide hydrogen and N-pyridine of piroxicam (Fig. 9). Another possibility is that the amide hydrogen may form a five-membered ring type of intramolecular hydrogen bond with the sulfonamide nitrogen (SO_2–N). The inter- and/or intramolecular hydrogen bonds may be able to weaken the N–H bond and cause the disappearance of the N–H stretching band.

Regarding the crystal structure of piroxicam, many inter- and intramolecular hydrogen bonds have been reported to exist in piroxicam forms I and II. These interactions cause the arrangement of piroxicam form I and II as dimers and infinite sheets, respectively (30,42). According to RDF analyses, the imidazole ring (both H–N_3 and N_1) of cimetidine can interact with functional groups in piroxicam. These interactions may

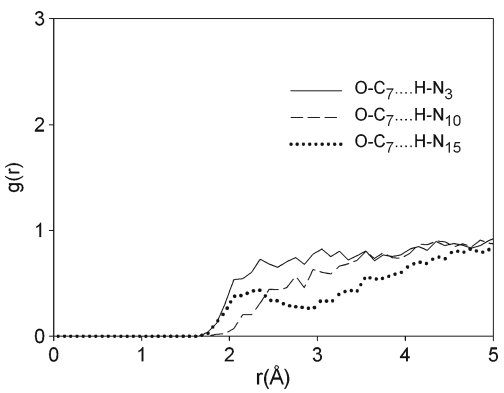

Fig. 8. Radial distribution functions for the piroxicam–cimetidine coprecipitate representing oxygen atom at C_7 of piroxicam (O–C_7) relative to the distance of the hydrogen atom at N_3-imidazole ring (H–N_3), N_{10} (H–N_{10}) and N_{15} (H–N_{15}) of cimetidine

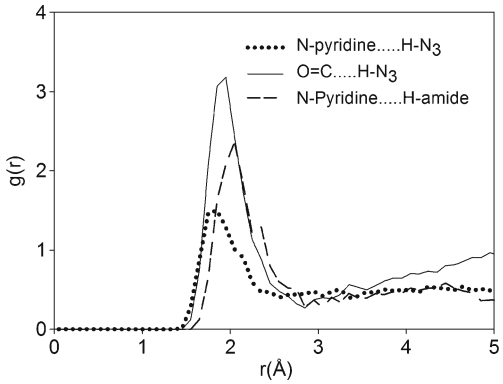

Fig. 9. Radial distribution functions (RDFs) for the piroxicam–cimetidine coprecipitate representing amide oxygen atom at C_9 (O═C) and pyridyl nitrogen (N-pyridine) atom of piroxicam relative to the distance of the hydrogen atom at N_3-imidazole ring (H–N_3) of cimetidine as well as RDF for pyridyl nitrogen and amide hydrogen of piroxicam

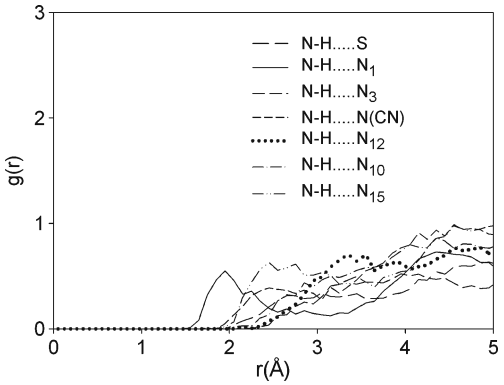

Fig. 11. Radial distribution functions for the piroxicam–cimetidine coprecipitate representing amide hydrogen atom at C_9 (N–H) of piroxicam relative to the distance of the S, N_1, N_3, N of CN group [N (CN)], N_{10}, N_{12}, and N_{15} of cimetidine

break the infinite chain of piroxicam form II in the coprecipitate and induce a conformational change which closely resembles that of piroxicam form I. Thus, an amorphous piroxicam in the coprecipitate contains some feature of piroxicam form I as demonstrated in its ^{13}C CP/MAS NMR.

The conformation of cimetidine form C was initially proposed to lie between the extended and bent structures using ^{13}C CP/MAS solid-state NMR (43). After this report, the small crystal structure of cimetidine form C was reinvestigated using high-resolution synchrotron powder diffraction, and the new data suggested an extended structure (44). According to the crystal structure of cimetidine form A, its conformation is in a "horseshoe" structure, in which the guanidinium proton (N_{15}–H) internally hydrogen bonds to the imidazole nitrogen (N_1) (43). This internal hydrogen bond is disrupted because the imidazole ring (N_1) of cimetidine interacts with piroxicam, as indicated by RDF analyses. Therefore, the folded structure of cimetidine form A is changed to the extended structure, similar to cimetidine form C, as observed in the C≡N stretching band in the FTIR spectrum of the coprecipitate.

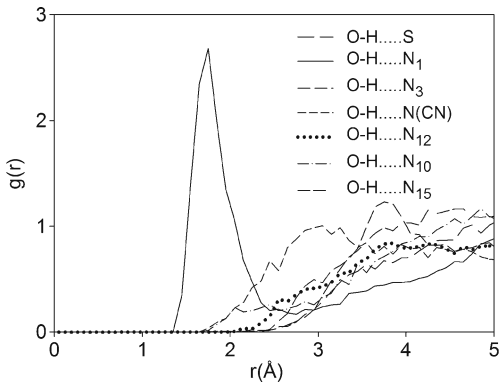

Fig. 10. Radial distribution functions for the piroxicam–cimetidine coprecipitate representing hydrogen atom at C_7 (O–H) of piroxicam relative to the distance of the S, N_1, N_3, N of CN group [N(CN)], N_{10}, N_{12} and N_{15} of cimetidine

CONCLUSIONS

In the coprecipitate, the initial crystalline forms of cimetidine form A and piroxicam form II were transformed to an amorphous form as observed using PXRD. In accordance with the FTIR spectra, the C≡N band in the coprecipitate is shifted from 2178 cm^{-1} to 2166 cm^{-1}, which corresponds to the C≡N band of cimetidine form C. This indicates that cimetidine in the coprecipitate has some features of cimetidine form C. According to the ^{13}C CP/MAS NMR spectra, the intermolecular interactions between piroxicam and cimetidine cause downfield shifts of C_{11}, C_{15}, and C_7 of piroxicam. The RDF analyses allowed us to identify the specific groups of piroxicam that interact with cimetidine. These include the pyridyl nitrogen of piroxicam with the H–N_3 cimetidine; the amide oxygen atom (C═O) of piroxicam with the H–N_3 cimetidine which is facilitated via electron delocalization from C_7; the hydrogen atom of OH–C_7 of piroxicam with the N_1 cimetidine. Thus, the imidazole ring of cimetidine is the major group that acts as a proton donor (H–N_3) and a proton acceptor (N_1) in the intermolecular interactions with the piroxicam molecule. The intermolecular interactions between these two drugs cause the transformation of the crystalline forms of the original drugs to an amorphous state, which may potentially change the physicochemical properties of the two drugs. To our knowledge, MD simulations have not been used to study the intermolecular interaction between amorphous drugs. This study demonstrates the successful approach of MD simulations for investigating the interaction of specific groups of amorphous drugs. Hence, this strategy may be useful for study of other amorphous systems of drugs.

ACKNOWLEDGMENTS

This work was supported by Prince of Songkla University, PSU-Grid and the National Nanotechnology Center (NANOTEC), National Science and Technology Development Agency (NSTDA), Ministry of Science and Technology through its National Nanoscience Consortium (CNC). The authors would like to thank Professor Terrence Cosgrove and Dr. Youssef Espidel for ^{13}C CP/MAS NMR experiments.

REFERENCES

1. Morre DJ, Morre DM. tNOX, an alternative target to COX-2 to explain the anticancer activities of non-steroidal anti-inflammatory drugs (NSAIDS). Mol Cell Biochem. 2006;283:159–67.
2. Knottenbelt C, Chambers G, Gault E, Argyle DJ. The in vitro effects of piroxicam and meloxicam on canine cell lines. J Small Anim Pract. 2006;47:14–20.
3. Semble EL, Wu WC. Antiinflammatory drugs and gastric mucosal damage. Semin Arthritis Rheum. 1987;16:271–86.
4. Finkelstein W, Isselbacher KJ. Drug therapy: cimetidine. N Engl J Med. 1978;299:992–6.
5. Maciel HP, Cardoso LG, Ferreira LR, Perazzo FF, Carvalho JC. Anti-inflammatory and ulcerogenic effects of indomethacin and tenoxicam in combination with cimetidine. Inflammopharmacol. 2004;12:203–10.
6. Takahashi HK, Watanabe T, Yokoyama A, Iwagaki H, Yoshino T, Tanaka N, *et al*. Cimetidine induces interleukin-18 production through H_2-agonist activity in monocytes. Mol Pharmacol. 2006;70:450–3.
7. Lefranc F, Yeaton P, Brotchi J, Kiss R. Cimetidine, an unexpected anti-tumor agent, and its potential for the treatment of glioblastoma (review). Int J Oncol. 2006;28:1021–30.
8. Milligan PA, McGill PE, Howden CW, Kelman AW, Whiting B. The consequences of H_2 receptor antagonist-piroxicam coadministration in patients with joint disorders. Eur J Clin Pharmacol. 1993;45:507–12.
9. Said SA, Foda AM. Influence of cimetidine on the pharmacokinetics of piroxicam in rat and man. Arzneimittelforschung. 1989;39:790–2.
10. Guo W, Hamilton JA. Phase behavior and crystalline structures of cholesteryl ester mixtures:A C-13 MASNMR study. Biophys J. 1995;68:2376–86.
11. Yamamura S, Gotoh H, Sakamoto Y, Momose Y. Physicochemical properties of amorphous salt of cimetidine and diflunisal system. Int J Pharm. 2002;241:213–21.
12. Hancock BC, Parks M. What is the true solubility advantage for amorphous pharmaceuticals? Pharm Res. 2000;17:397–404.
13. Liu J, Qiu L, Gao J, Jin Y. Preparation, characterization and in vivo evaluation of formulation of baicalein with hydroxypropyl-beta-cyclodextrin. Int J Pharm. 2006;312:137–43.
14. Zmitek J, Smidovnik A, Fir M, Prosek M, Zmitek K, Walczak J, *et al*. Relative bioavailability of two forms of a novel water-soluble coenzyme Q10. Ann Nutr Metab. 2008;52:281–7.
15. Tantishaiyakul V, Kaewnopparat N, Ingkatawornwong S. Properties of solid dispersions of piroxicam in polyvinylpyrrolidone K-30. Int J Pharm. 1996;143:59–66.
16. Tantishaiyakul V, Kaewnopparat N, Ingkatawornwong S. Properties of solid dispersions of piroxicam in polyvinylpyrrolidone. Int J Pharm. 1999;181:143–51.
17. Valizadeh H, Zakeri-Milani P, Barzegar-Jalali M, Mohammadi G, Danesh-Bahreini MA, Adibkia K, *et al*. Preparation and characterization of solid dispersions of piroxicam with hydrophilic carriers. Drug Dev Ind Pharm. 2007;33:45–56.
18. Redenti E, Zanol M, Ventura P, Fronza G, Comotti A, Taddei P, *et al*. Raman and solid state ^{13}C-NMR investigation of the structure of the 1:1 amorphous piroxicam:β-cyclodextrin inclusion compound. Biospectroscopy. 1999;5:243–51.
19. Tantishaiyakul V, Songkro S, Suknuntha K, Permkum P, Pipatwarakul P. Crystal structure transformations and dissolution studies of cimetidine–piroxicam coprecipitates and physical mixtures. AAPS PharmSciTech. 2009;10:789–95.
20. Okonogi S, Puttipipatkhachorn S. Dissolution improvement of high drug-loaded solid dispersion. AAPS PharmSciTech. 2006;7: E1–6.
21. Mashru RC, Sutariya VB, Sankalia MG, Yagnakumar P. Characterization of solid dispersions of rofecoxib using differential scanning calorimeter. JTherm Anal Calorim. 2005;82: 167–70.
22. Schachter DM, Xiong J, Tirol GC. Solid state NMR perspective of drug-polymer solid solutions: a model system based on poly (ethylene oxide). Int J Pharm. 2004;281:89–101.
23. Suknuntha K, Tantishaiyakul V, Vao-Soongnern V, Espidel Y, Cosgrove T. Molecular modeling simulation and experimental measurements to characterize chitosan and poly(vinyl pyrrolidone) blend interactions. J Polym Sci Polym Phys. 2008;46:1258–64.
24. Sandoval C, Castro C, Gargallo L, Radic D, Freire J. Specific interactions in blends containing chitosan and functionalized polymers. Molecular dynamics simulations. Polymer. 2005;46:10437–42.
25. Suga Y, Takahama T. Application of molecular simulation to prediction of solubility parameter. Chem Lett. 1996;281–2.
26. Jacobson SH. Molecular modeling studies of polymeric transdermal adhesives: structure and transport mechanisms. Pharm Technol. 1999;122–30.
27. Li B, Pan F, Fang Z, Liu L, Jiang Z. Molecular dynamics simulation of diffusion behavior of benzene/water in PDMS-calix [4] arene hybrid pervaporation membranes. Ind Eng Chem Res. 2008;47:4440–7.
28. Heuchel M, Hofmann D, Pullumbi P. Molecular modeling of small-molecule permeation in polyimides and its correlation to free-volume distributions. Macromolecules. 2004;37:201–14.
29. Vrecer F, Vrbinc M, Meden A. Characterization of piroxicam crystal modifications. Int J Pharm. 2003;256:3–15.
30. Sheth AR, Bates S, Muller FX, Grant DJW. Polymorphism in piroxicam. Cryst Growth Des. 2004;4:1091–8.
31. Baranska M, Proniewicz LM. FT-IR and FT-Raman spectra of cimetidine and its metallocomplexes. J Mol Struct. 1999;511–512:153–62.
32. Shibata M, Kokubo H, Morimoto K, Morisaka K, Ishida T, Inoue M. X-ray structural studies and physicochemical properties of cimetidine polymorphism. J Pharm Sci. 1983;72:1436–42.
33. Sheth AR, Bates S, Muller FX, Grant DJW. Local structure in amorphous phases of piroxicam from powder X-ray diffractometry. Cryst Growth Des. 2005;5:571–8.
34. Rigby D. Fluid density predictions using the COMPASS force field. Fluid Phase Equilib. 2004;217:77–87.
35. Mazeau K, Heux L. Molecular dynamics simulations of bulk native crystalline and amorphous structures of cellulose. J Phys Chem B. 2003;107:2394–403.
36. Tantishaiyakul V, Permkam P, Suknuntha K. Use of DRIFTS and PLS for the determination of polymorphs of piroxicam alone and in combination with pharmaceutical excipients: a technical note. AAPS PharmSciTech. 2008;9:95–9.
37. Hegedus B, Gorog S. The polymorphism of cimetidine. J Pharm Biomed Anal. 1985;3:303–13.
38. Middleton DA, Duff CSL, Berst F, Reid DG. A cross-polarization magic-angle spinning 13C NMR characterization of the stable solid-state forms of cimetidine. J Pharm Sci. 1997;86:1400–2.
39. Sheth AR, Lubach JW, Munson EJ, Muller FX, Grant DJW. Mechanochromism of piroxicam accompanied by intermolecular proton transfer probed by spectroscopic methods and solid-phase changes. J Am Chem Soc. 2005;127:6641–51.
40. Geckle JM, Rescek DM, Whipple EB. Zwitterionic piroxicam in polar solution. Magn Reson Chem. 1989;27:150–4.
41. Karpinska G, Dobrowolski JC, Mazurek AP. Conformation and tautomerism of the cimetidine molecule: a theoretical study. J Mol Struct. 2003;645:37–43.
42. Taddei P, Torreggiani A, Simoni R. Influence of environment on piroxicam polymorphism: vibrational spectroscopic study. Biopolymers. 2000;62:68–78.
43. Middleton DA, Duff CSL, Peng X, Reid DG, Saunders D. Molecular conformations of the polymorphic forms of cimetidine from ^{13}C solid-state NMR distance and angle measurements. J Am Chem Soc. 2000;122:1161–70.
44. Birkedal H, Bauer-Brandl A, Pattison P. The surprising polymorph C of cimetidine: synchrotron radiation to the rescue. *XIXth European Crystallographic Meeting*. Nancy, France: Abstracts. Acta Cryst. 2000;A56:s337. Supplement.